COMPDYN 2013
4th ECCOMAS Thematic Conference on
Computational Methods in Structural Dynamics and Earthquake Engineering
M. Papadrakakis, V. Papadopoulos, V. Plevris (eds.)
Kos Island, Greece, 12–14 June 2013

EMULATIVE COLUMN-FOOTING CONNECTIONS FOR SEISMIC DESIGN IN ACCELERATED BRIDGE CONSTRUCTION

Zachary B. Haber[1], M. Saiid Saiidi[2], and David Sanders[3]

University of Nevada, Reno
1664 N. Virginia St. MS. 258, Reno, NV 89512
[1]e-mail: zhaber@unr.edu
[2]e-mail: saiidi@unr.edu
[3]e-mail: sanders@unr.edu

Keywords: Mechanical splice, ductility, precast, cyclic loading, damage

Abstract. *Accelerated bridge construction (ABC) is gaining substantial momentum in the US because of its many advantages. Extensive use of precast members is necessary for ABC to succeed. Some of the key advantages of ABC are: (1) higher quality of construction for structural elements because of fabrication in plants, (2) more durable materials because of more appropriate curing in plants, (3) concurrent execution of different tasks, (4) reduced traffic interruption and less risk to the traveling public and construction crew, and (5) reduced direct and indirect effect on the environment due to expedited construction and the use of more efficient technologies that require less energy. Despite their numerous advantages prefabricated columns have rarely been used in areas of high seismicity because of high uncertainty about their seismic performance.*

Extensive effort has been in progress at the University of Nevada, Reno to develop and evaluate earthquake resistant connections for use in accelerated bridge construction. This effort included the study of five half-scale bridge column models that were constructed and tested under reversed slow cyclic loading. The study focused on developing four new moment connections at column-footing joints for accelerated bridge construction in regions of high seismicity. The new connections were employed in precast columns each utilizing mechanical splices to create connectivity with reinforcing bars in a cast-in-place footing. Two different mechanical splices were studied; an upset headed coupler and grout-filled sleeve coupler. Along with the splice type, the location of splices within the plastic hinge zone was also a test variable. All precast models were designed to emulate conventional cast-in-place construction thus were compared to a conventional cast-in-place test model. Results indicate that the new connections are promising and duplicate conventional cast-in-place construction with respect to key response parameters although the plastic hinge mechanism could be significantly affected by the presence of splices.

1 INTRODUCTION

Accelerated bridge construction (ABC) has become increasingly popular throughout the United States because of its numerous advantages. In many cases, ABC methodologies have been shown to decrease bridge construction time and reduce the overall project cost. To effectively execute ABC projects, designers use prefabricated structural elements that can be manufactured offsite in parallel with on-site construction, which can result in improved element quality. These members are then delivered to the site and can be quickly assembled to form a functional structural system. It is advantageous to the bridge designer if ABC systems emulate conventional cast-in-place construction systems because this would allow typical analysis and design procedures to be used. The difficulty with developing emulative systems is usually encountered in designing connections because of their critical role in transferring forces from the superstructure to the foundation. Substructure connections are particularly critical in high seismic zones because they must dissipate energy through significant cyclic nonlinear deformations while maintaining capacity and stability of the structural system.

There have been a limited number of studies conducted on substructure connections for ABC projects in seismic zones. A summary of different connection details for moderate-to-high seismic zones is presented in the work by Marsh et al., 2011. Many of the connections mentioned in this literature survey were evaluated experimentally and include grouted duct connections (Restrepo et al., 2011), pocket-type connections (Restrepo et al., 2011), and column-in-socket connections (Motaref et al., 2011). The performance of these connections were comparable to cast-in-place baseline models but may require unconventional design procedures or detailing requirements. Mechanically spliced connections could provide emulative behavior without deviating substantially from conventional design procedures and details. There are only a limited number of studies that have been conducted on using these devices in plastic hinge zones (Hironobu et al., 2005; Huang et al., 1997; Lehman et al., 2001; and Reetz et al., 2004)

These previous studies do not provide information as to how mechanical splices can be used to design and construct precast bridge columns that conform to US standards. An experimental study was conducted at the University of Nevada, Reno to investigate the performance of these devices in moment connections between precast columns and cast-in-place (CIP) footings by testing five large-scale models under cyclic loading. This paper highlights the key aspects of study and the results. A detailed description of this study can be found in Haber et al., 2013.

2 HALF-SCALE BRIDGE COLUMN MODELS

Five half-scale reinforced concrete bridge column models with circular sections were investigated in this study: one conventional cast-in-place (CIP) benchmark column and four precast columns. The models were identical except for the details in the plastic hinge connection region. The benchmark column was designed using the California Department of Transportation (Caltrans) Seismic Design Criteria (SDC) (Caltrans, 2010) for a target design displacement ductility of $\mu_D = 7.0$ to achieve large inelastic deformations prior to failure. The geometry and reinforcement details of CIP were selected to be representative of flexural-dominate columns commonly used in California with modern seismic detailing. CIP was reinforced with eleven evenly-distributed D25 [No. 8] bars in the longitudinal direction and a D10 [No. 3] spiral with a 51 mm [2 in] pitch. These reinforcement details correspond to reinforcement ratios of approximately 2% and 1% in the longitudinal and transverse directions, respectively. The design axial load was taken as 10% the nominal axial load capacity of the

gross concrete area of the column, which was 1005 kN [226 kips]. CIP was half-scale, with a 610-mm [24-in] diameter, assuming a 1220-mm [48-in] diameter prototype, and was 2743 mm [108 in] in height from the surface of the footing to lateral loading point. A rectangular reinforced concrete head atop each column was used to transfer lateral load from the actuator. The footings were designed to remain elastic and were post-tensioned to the strong floor to prevent sliding and over-turning under lateral loads. Figure 1-a depicts the general geometry and reinforcement configuration for the column cage of CIP.

The remaining four models were precast and utilized a hollow concrete shell that contained the same longitudinal and transverse reinforcement as CIP. Once the precast column shells were connected to the footing, the core was filled with self-consolidating concrete (SCC). The connection of the precast column shell to the footing was achieved by using mechanical bar couplers. Two different connection details were developed using two different mechanical reinforcing bar splices. The first detail (Figure 1-b) employed the use of upset headed couplers to make the connection between the longitudinal steel in the precast column shell and that embedded within the footing. This connection was made by lowering the column shell onto the footing then joining the two elements with transition reinforcing bars. Once the transition bars were locked in place, the transverse steel spiral was tied into place. Finally, formwork was constructed and the connection was completed by pumping cementitious grout to cover the connection region area. The second connection detail (Figure 1-c) utilized ductile cast-iron grout filled sleeves to connect the column shell to the footing. The connection between the shell and footing was achieved by lowering the shell onto bar dowels that protruded from the footing. Once the shell was lowered onto the dowels, each sleeve was pressure grouted through plastic ducts that protruded from the column shell. The grout used was a high strength (100+ MPa) proprietary mix that was supplied by the grout sleeve manufacturer. Two column models were tested for each connection detail; one where the connection was made directly to the footing and the second where the column was mounted on a 305-mm [12-in] precast pedestal (Figure 1-d), which was used to reduce the moment demand over the connection location. Longitudinal reinforcing bar passed though the pedestals via grout-filled corrugated steel ducts. Column models were denoted by the type of coupler ("HC" for headed coupler and "GC" for grouted coupler) and whether the model included a pedestal ("NP" for no pedestal and "PP" for precast pedestal).

(a) (b) (c) (d)

Figure 1: Experimental models: (a) Details of the benchmark column (CIP); (b) Connection region of HCNP; (c) Connection region of GCNP; (d) Precast pedestal for GCPP

3 EXPERIMENTAL METHODS

Each column model was instrumented with several layers of foil-backed resistive strain gages installed on the longitudinal and transverse reinforcing bars. String pot and linear variable displacement transducers (LVDT) were used to record the column head displacement, plastic hinge curvatures, bond-slip at the base of the column, and rotations at the column-to-pedestal joint. Tests were conducted at the Large-scale Structures Laboratory at the University of Nevada, Reno using a single cantilever loading configuration. Lateral load was applied with a 978 kN [220 kip] servo-controlled hydraulic actuator that was mounted to a reaction pylon. Column models were subjected to slow cyclic loading using a drift-based displacement-control loading protocol. Two full push and pull cycles were completed at drift levels of 0.25, 0.5, 0.75, 1, 2, 3, 4, 5, 6, 8, and 10% until failure, defined to be a drop in lateral. A nominally constant axial load of 890 kN [200 kip] was applied to each column model using two hydraulic rams and a spreader beam.

3.1 Force-Deformation Behavior

The measured force-displacement relationships for the precast models HCNP and GCNP are plotted along with that of CIP in Figure 2; models with precast pedestals behavior similar to the counterparts without pedestals. CIP exhibited wide loops, stable post-yield regions, and minimal strength degradation, as expected for a column with modern seismic detailing. The measured response of HCNP was approximately the same as that of CIP except for slight differences in peak load per drift level and pinching during unloading. The reason for the pinching is as follows: when longitudinal bars are under tension, the headed ends within the threaded splice collars separate and a gap is formed. Upon reversal of the load, these bars move toward each other, but a compressive force is developed only after the gap is closed. The column displaces slightly to close this gap, which leads to a pinch. Although this behavior is clearly observable, the path of the hysteresis loop varies only slightly from that of CIP. The first abrupt drop in lateral load occurred during the second cycle of -10% drift in both models. The same pinching behavior was seen in the response of HCPP but did not cause significant deviation in the loops when compared to CIP. The measured response of GC models was also similar to that of CIP. Figure 2-b shows a comparison between the GCNP and CIP. The primary difference between CIP and the GC models was the drift capacity. CIP completed one full cycle at the 10% drift ratio prior to loss of lateral load capacity while GCNP and GCPP experienced abrupt loss during the 6% drift cycles.

The envelopes of the measured force-displacement relationships are shown in Figure 3. The curves represent the average envelope from the first cycle of the push-pull loadings. In all cases, the envelope curves for the precast models were comparable with CIP. The initial stiffness up to a lateral load of 156 kN [35 kips] was the same among the five models at which point the stiffness of HCPP decreased slightly. At a lateral load of 236 kN [53 kips], GCPP began to soften due to yielding and subsequently followed a path similar to that of HCPP. The paths of HCNP and GCNP did not deviate from CIP until approximately 2.5% drift which corresponded to spalling of cover concrete. Despite these subtle differences, all five curves exhibited similar ascending braches, stable post-yield plateaus, and achieved approximately that same lateral load capacity.

Figure 3 also shows the displacement ductility achieved by each model. In all cases the displacement ductility capacity was satisfactory. That is, CIP and the HC models achieved ductility within 0.5 of the target design ductility of 7.0. The GC models both failed at displacement ductility 4.5. Although this was 35% lower than the target design ductility it would be sufficient in regions with moderate to high seismicity.

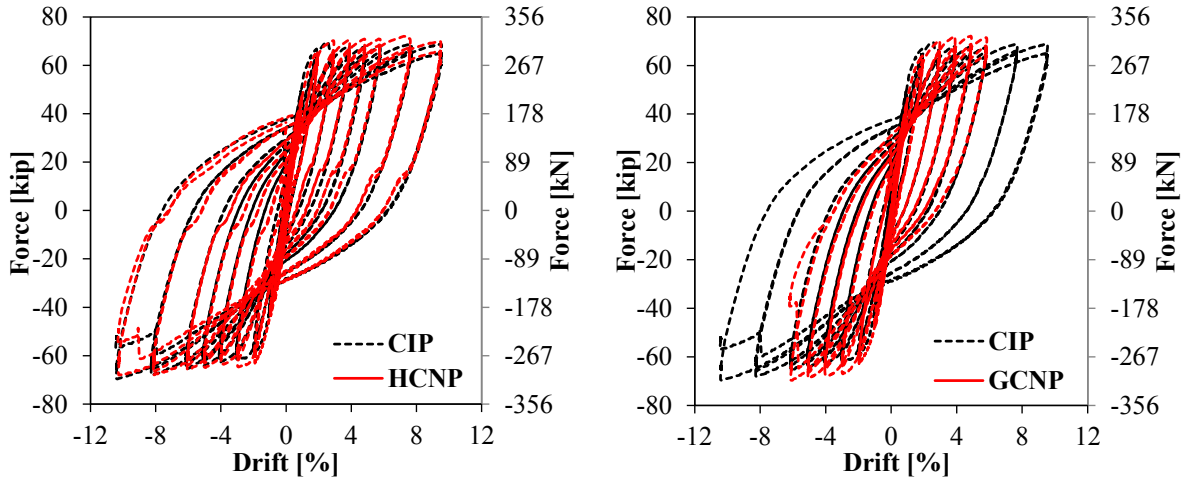

(a) Comparison between CIP and HCNP (b) Comparison between CIP and GCNP

Figure 2: Hysteretic force-displacement relationships

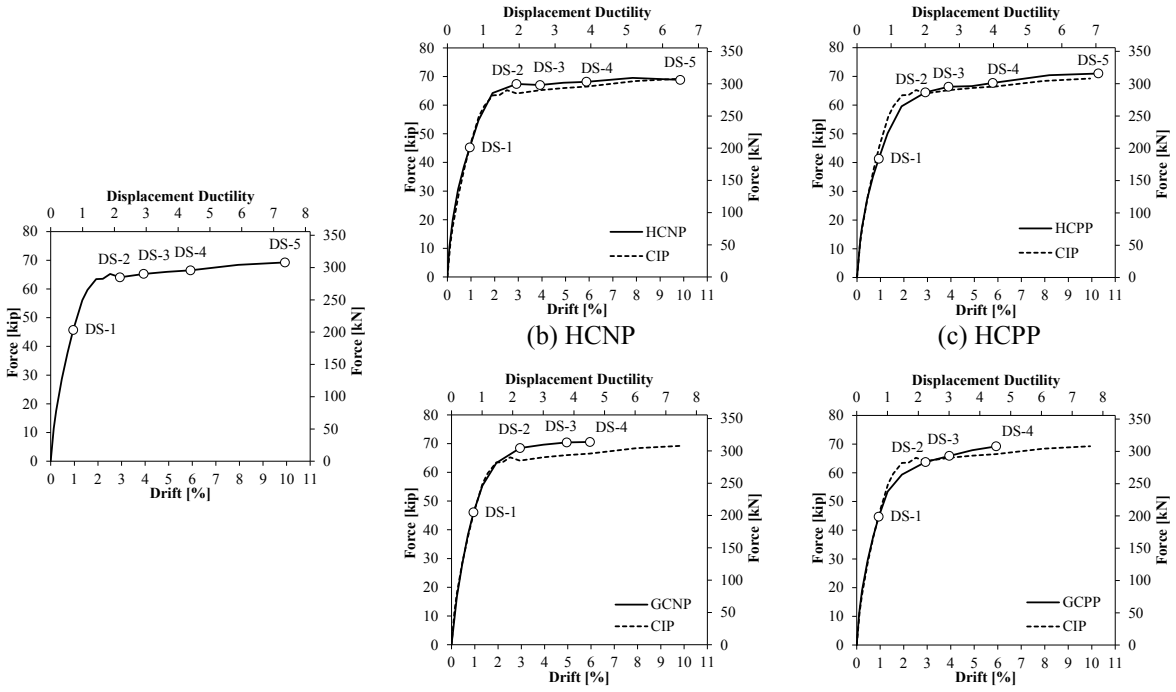

(a) Cast-in-place (CIP) (b) HCNP (c) HCPP (d) GCNP (e) GCPP

Figure 3: Average envelope curves

3.2 Apparent Damage and Failure

The progression of damage in the precast models was similar to that of CIP. The damage progression of each model was evaluated by first defining five distinct damage states (DS). The damage state corresponded to presence of flexural cracks (DS-1), first spall and development of shear cracks (DS-2), extensive cracking and spalling of concrete (DS-3), visible longitudinal and/or transverse reinforcement (DS-4), and on-set of confined concrete core damage (DS-5: imminent failure). Figure 4 illustrates each damage state as observed in CIP. The progression of damage for each model is depicted on the average envelope curves shown in Figure 3. The HC models reached all five damages, which occurred at approximately the same point in the force-displacement history as CIP. The GC models achieved damages states DS-1 through DS-4 prior to failure, which occurred at 6% drift. The progression of damage

for the GC models was the same as CIP except for DS-3 in GCNP, which occurred at a later drift ratio.

All five models exhibited cracking and delamination of concrete at the footing surface due to strain penetration of the longitudinal bar. Yet, the extent of this damage was much greater in the GC models compared to CIP and the HC models. By 6% drift, severe damage to the footing was observed in both GCNP and GCPP, which included extensive cracking and delamination of concrete. The loss of the surrounding concrete in the footing resulted in buckling of longitudinal bars and their eventual fracture. This level of damage in the footing was not observed the HC models or CIP until 8.0% drift.

To determine the failure mechanism and location, concrete was removed from the plastic hinge region and footing of each model. It was determined that the dominant failure mode in all models was longitudinal bar fracture. Ruptured bars where found 76-254 mm [3-10 in] above the footing in CIP and HCNP, and approximately 102-127 mm [4-5 in] below the surface of the footing in the other models. It was concluded that bar rupture below the footing surface was caused by strain concentrations that developed as a results of the presence of the grouted pedestal ducts and cast-iron grouted coupler sleeves.

In order to assess possible damage, mechanical splices were removed from HCNP and GCNP because they were subjected to the highest moment demand and inelastic deformations. The upset-headed splice did not display any indication of distress or damage. However there was slack between the deformed heads within the threaded splice collar, which is likely associated with permanent localized deformations within the splice collar. The grouted-sleeves removed from GCNP did not exhibit any damage and the bond between the high-strength grout and reinforcing bar was sound. There was, however, evidence of strain penetration into the coupler sleeve as shallow grout-cone pull-out was observed at both ends.

(a) DS-1 (b) DS-2 (c) DS-3 (d) DS-4 (e) DS-5

Figure 4: Apparent damage states

3.3 Plastic Hinge Behavior

The plastic hinge behavior of each model was evaluated using longitudinal reinforcing bar strains and rotations measured within the first 1.5 column diameters above the footing. CIP exhibited well distributed strain throughout the plastic hinge, which resulted in a large region where plastic rotation occurred. HCNP also displayed well distributed strains throughout the plastic hinge region and the magnitude of the strains were approximately the same as CIP. Conversely, the measured distributions of strain for the HCPP and the GC models were not as uniform as those for CIP and HCNP. For HCPP and the GC models, maximum tensile strains occurred within the footing, which was consistent with the observed longitudinal bar rupture locations. Furthermore, large plastic strains were also measured at the column-pedestal interface for HCPP and GCPP. For these models, the tensile strains occurring within the pedestal were not as substantial as those occurring at the joints due to the additional stiffness provided

by the grout-filled corrugated steel ducts. These observations indicate that the plastic hinge behavior of the columns was altered by presence of the grouted coupler and the precast pedestals.

The change in plastic hinge behavior can be further quantified by comparing the moment-rotation relationships for CIP and GCNP, which represents the most extreme difference. Figure 5 depicts the moment-rotation relationships that were measured for CIP and GCNP. It can be observed that within the first half column diameter (approximately) above the footing, CIP (Fig. 5-a) exhibits significantly more plastic rotation than GCNP (Fig. 5-b). The presence of the grouted coupler sleeves increased the section stiffness within this region resulting in reduced plastic rotation. It can be observed in Figures 5-c and –d, which depict the moment-rotation relationships for the region within the second half column diameter, that the plastic rotation for GCNP exceeds that of CIP. This further confirms that hinge shifting is occurring.

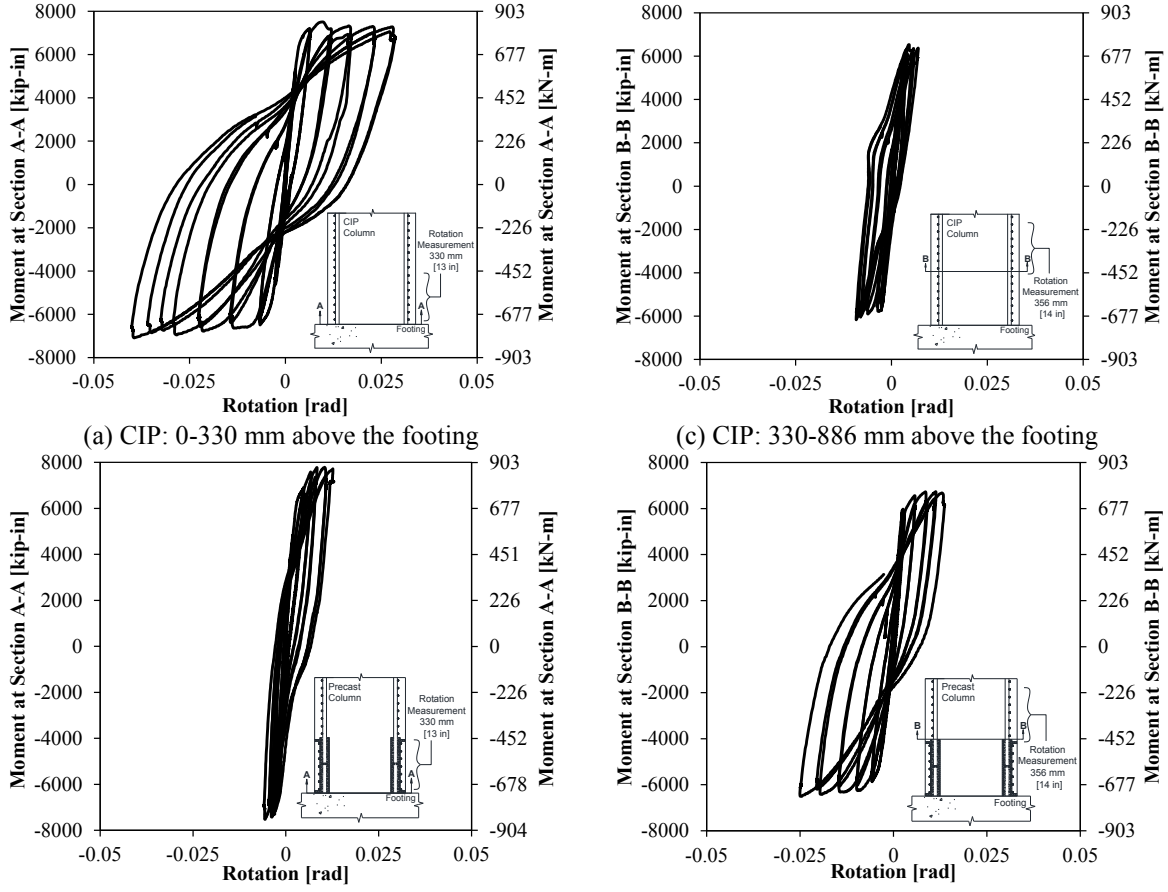

(a) CIP: 0-330 mm above the footing

(c) CIP: 330-886 mm above the footing

(b) GCNP: 0-330 mm above the footing

(d) GCNP: 330-886 mm above the footing

Figure 5: Hinge rotation comparison between CIP and GCNP

4 SUMMARY AND CONCLUSIONS

The study presented in this paper focused on evaluating the seismic performance of four emulative precast column-to-footing connections which utilized mechanical reinforcing bar. A set of geometric and reinforcement details were developed using a half-scale benchmark column such that two different mechanical splices could be incorporated into the plastic hinge zone reinforcement details. The benchmark design details were also used to construct conventional cast-in-place (CIP) column model that served as the baseline for evaluating the performance of precast models. Four precast column models were constructed with different

plastic hinge connection details: Two were connected directly to the footing (HCNP and GCNP), and two were connected atop a precast pedestal one-half column diameter in height (HCPP and GCPP).

A number of similarities were found between the behavior of CIP and the precast models. All models exhibited hysteresis loops that were wide and stable, similar average force-displacement envelope curves, and all three models had approximately the same ultimate lateral load capacity. The damage accumulated by each model at the various drift level was also similar. The main difference between the CIP and the precast models was observed in GCNP and models with precast pedestals; a distinct difference in the plastic hinge behavior was observed. The hinge region in CIP allowed for plastic deformation to occur evenly throughout the section whereas HCPP, GCNP, and GCPP forced this deformation to occur at pedetsal joints and within the footing.

It can be concluded that the behavior of the connections tested in this study are emulative of conventional cast-in-place construction except there where some difference in displacement ductility capacity. The presence of the grouted couplers and precast pedestals in the plastic hinge forced a large amount of plastic deformations within the footing, which ultimately resulted in longitudinal bar fracture. Nevertheless, the displacement ductility achieved by each of the precast models was sufficient for construction in moderate and high seismic zones.

REFERENCES

[1] Marsh, M. L., Wernli, M., Garrett, B. E.; Stanton, J. F.; Eberhard, M. O.; and Weinert, M. D., "Application of Accelerated Bridge Construction Connections in Moderate-to-High Seismic Region," *NCHRP Report 698*, pp. 65, 2011.

[2] Restrepo, J. I., Tobolski, M. J., and Matsumoto, E. E., "Development of a Precast Bent Cap System for Seismic Regions," *NCHRP Report 681*, pp. 116, 2011.

[3] Motaref, S., Saiidi, M., and Sanders, D. H., "Seismic Response of Precast Bridge Columns with Energy Dissipating Joints," *Report No. CCEER-11-01*, Center for Civil Engineering Earthquake Research, pp. 760, 2011.

[4] Hironobu, A. et al., "Cyclic Loading Experiment of Precast Columns of Railway Rigid-Frame Viaduct Installed with NMB Splice Sleeves," *Proceedings of the Japan Concrete Institute*, V. 27, No. 2, 2005.

[5] Huang, S .W., Yu, J. T., Chiou, H. D., Asakawa, T., and Tsai, K. C., "Final report of experiment on precast reinforced concrete beam-column assemblage," *Chinese Society of Structural Engineering*. 2011.

[6] Lehman, D. E., Gookin, S. E., Nacamuli, A. M., and Moehle, J. P., "Repair of Earthquake-Damaged Bridge Columns," *ACI Structural Journal*, V. 98, No. 2, 2001.

[7] Reetz, R. J., Ramin, M. V., and Matamoros, A., "Performance of Mechanical Splices within the Plastic Hinge Region of Beams Subject to Cyclic Loading," *Proceeding of the 13th World Conference on Earthquake Engineering*, August 1-6, 2004.

[8] Haber, Z. B., Saiidi, M., and Sanders, D. H., "Precast Column-Footing Connection for Accelerated Bridge Construction in Seismic Zones," Center for Civil Engineering Earthquake Research, Department of Civil and Environmental Engineering, University of Nevada, Reno, Nevada, *Report No. CCEER-##-13*, In Preparation, 2013.

[9] California Department of Transportation, "*Seismic Design Criteria (SDC) Version 1.6*," Division of Engineering Services, Sacramento, Calif., pp. 160, 2010.